CHEMBIOCHEM

DOI: 10.1002/cbic.200900758

Substrate Conformations Set the Rate of Enzymatic Acrylation by Lipases

Per-Olof Syrén and Karl Hult*[a]

Acrylates represent a class of α,β-unsaturated compounds of high industrial importance. We investigated the influence of substrate conformations on the experimentally determined reaction rates of the enzyme-catalysed transacylation of methyl acrylate and derivatives by ab initio DFT B3LYP calculations and molecular dynamics simulations. The results supported a least-motion mechanism upon the sp^2 to sp^3 substrate transition to reach the transition state in the enzyme active site. This was in accordance with our hypothesis that acrylates form productive transition states from their low-energy s-*sis*/s-*trans* conformations. Apparent k_{cat} values were measured for *Candida antarctica* lipase B (CALB), *Humicola insolens* cutinase and *Rhizomucor miehei* lipase and were compared to results from computer simulations. More potent enzymes for acryltransfer, such as the CALB mutant V190A and acrylates with higher turnover numbers, showed elevated populations of productive transition states.

Introduction

Acrylates are α,β-unsaturated esters that are used as monomeric starting materials for a wide range of commercial applications such as coatings, plastics and paints. The double bond present in this class of molecules is useful for cross-linking purposes by radical polymerisation. Esters of acrylic acid or methacrylic acid are traditionally made chemically under harsh reaction conditions with sulfuric acid as catalyst.[1] It is necessary to add polymerisation inhibitors for processes run at elevated temperatures.

Biocatalysis is a "green", sustainable alternative to traditional chemistry. Enzymes can be used under mild reaction conditions and they show high activity and regio- and stereo selectivity. Lipases are of industrial interest due to their high stability in organic media, substrate tolerance and stereoselectivity.[2] Regioselective transacylation of ethyl acrylate with sterically hindered diols to obtain the monoester by using lipase from *Chromobacterium viscosum* has been described in the literature.[3] Lipase B from *Candida antarctica* (CALB, also known as *Pseudozyma antarctica* lipase B) showed the best catalytic performance in the transacylation of methyl acrylate with undecan-1-ol out of 19 enzymes tested.[4] Monoacrylation of polyols with CALB has been described in a patent from BASF.[5] The influence of solvent choice and water activity on the reaction rate of lipase-catalysed transacylation of acrylic acid and ethyl acrylate has been reported.[6] One problem with chemical and enzymatic transacylations of acrylates is the low reaction rate. To our knowledge, no attempts have been made to explain this fact.

Acrylates have been shown to exist in two conformations, s-*cis* and s-*trans*, Scheme 1, with a high rotational barrier to isomerisation.[7] This can be explained by the stabilising interaction between the π orbitals of the alkene group and the carbonyl double bond.

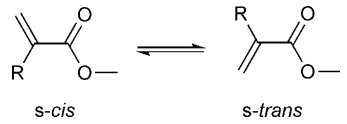

Scheme 1. The two possible acrylate conformers.

In this study we have investigated the distribution of different substrate conformers of methyl acrylate and derivatives by using ab initio calculations. The influence of substrate conformational distribution on the experimentally determined reaction rate of enzyme-catalysed transacylation was investigated by molecular dynamics simulations. Thus both the relative abundance of free substrate conformers and how well these conformers fit in the active site were considered. CALB wt (EC 3.1.1.3) and mutant V190A, *Rhizomucor miehei* lipase (RML, EC 3.1.1.3) and cutinase from *Humicola insolens* (HiC, EC 3.1.1.74) were analysed. The aim of this work was to get a deeper understanding of enzyme-catalysed acryltransfer. The gained knowledge can be used for in silico protein design of lipase variants with increased activity towards acrylate substrates as a complement to traditional laboratory work (mutant library construction and screening). The results were in agreement with our hypothesis that acrylates mainly react in their low-energy, ground state, s-*cis*/s-*trans* conformations.

[a] *P.-O. Syrén, Prof. K. Hult*
Department of Biochemistry, School of Biotechnology
Royal Institute of Technology, AlbaNova University Center
10691 Stockholm (Sweden)
Fax: (+46) 8-5537-8468
E-mail: kalle@biotech.kth.se

Supporting information for this article is available on the WWW under http://dx.doi.org/10.1002/cbic.200900758.

Results and Discussion

The view on how enzymes can achieve their remarkable rate acceleration compared to the corresponding reaction in solution has changed a lot since the lock-and-key model was introduced by Emil Fisher.[8] Clearly, enzymes are not rigid catalysts, and the important factors for catalysis include proximity effects, electrostatic stabilisation of the transition state (TS), symmetrical hydrogen bonds and tunnelling.[9] For acrylates there is a stabilising π system in the free substrate that can affect catalysis. Our hypothesis that the reaction rate for enzyme-catalysed transacylation of acrylates is determined by the ability of ground state s-*cis*/s-*trans* conformations of the free acrylate substrates to form transition states was evaluated by kinetic experiments and computer modelling.

The experimentally determined apparent k_{cat} values for transacylation with the saturated ester methyl propionate and the α,β-unsaturated compounds methyl acrylate, methyl methacrylate and methyl α-chloroacrylate in diisopropyl ether at a concentration of propan-1-ol of 25 mM are given in Table 1.

Table 1. Experimentally determined apparent k_{cat} values when using 25 mM propan-1-ol as acyl acceptor in diisopropyl ether at 30 °C.

	CALB[a] wt [min^{-1}]	CALB V190A [min^{-1}]	HiC[b] [min^{-1}]	RML[c] [min^{-1}]
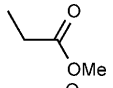	2000	1000	1000	3000
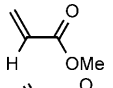	510	240	170	40
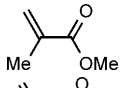	60	170	80	50
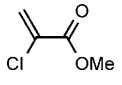	250	520	280	120

[a] *Candida antarctica* lipase B. [b] *Humicola insolens* cutinase. [c] *Rhizomucor miehei* lipase.

The presence of the α,β-double bond in methyl acrylate leads to a reduction in apparent k_{cat} of 4–75 times compared to that of methyl propionate depending on the enzyme. Methyl methacrylate reacted even more slowly with an additional reduction in apparent k_{cat} of ten times for CALB wt. Methyl α-chloroacrylate represents an activated compound with increased reactivity compared to methyl methacrylate, indicative of an electronic effect due to the fact that the chloro and methyl groups are approximately isosteric. Interestingly, *Rhizomucor miehei* lipase had the same apparent k_{cat} for methyl methacrylate and methyl acrylate.

The distribution of substrate conformers for the different acrylates was analysed by DFT B3LYP ab initio calculations with the 6−311+G(2d,2p) basis set (Table 2). The geometry-optimised structures were found to be either s-*cis* or s-*trans* conformers. The barrier to s-*cis*/s-*trans* isomerisation of methyl acrylate was calculated to be 6 kcal mol^{-1} at this level of theory.

Table 2. Population analysis of substrates by using DFT at the B3LYP 6−311+G(2d,2p) level of theory.

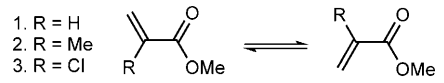

s-*cis* s-*trans*

	$E_{rel,PCM}$ [kcal mol^{-1}][a]		Relative abundance[b]	
	s-cis	*s-trans*	*s-cis*	*s-trans*
1	0.0	0.6	0.73	0.27
2	0.6	0.0	0.27	0.73
3	0.0	0.2	0.58	0.42

[a] The relative energies with solvation were taken into account by using the CPCM polarisable continuum model with diethyl ether ($\varepsilon = 4.335$). [b] Relative abundances are given at 302 K in diethyl ether.

A DFT B3LYP 6−31G(d,p) single-point calculation on methyl acrylate with perpendicular π orbitals resulted in an energy that was 7 kcal mol^{-1} higher than that of the low-energy s-*cis* conformation. The single-point energy was thus in good agreement with the calculated barrier at the higher level of theory. The corresponding single-point energies for methyl methacrylate and methyl α-chloroacrylate with perpendicular π orbitals were found to be 6 kcal mol^{-1} higher than the energies for their respective low-energy conformation (see Table S5 in the Supporting Information). The calculated barriers for isomerisation were thus found to be much smaller than the barriers for transacylation (17 kcal mol^{-1} for methylacrylate with CALB at 303 K based on the apparent k_{cat} value given in Table 1). The enzyme will thus encounter a constant concentration of s-*cis*/s-*trans* acrylate conformers.

A dihedral angle of 15° between the carbonyl and alkene double bonds, which represents a small perturbation of the π system, resulted in an energy increase of 0.3–0.4 kcal mol^{-1} (Table S5). It was concluded that distortion of the π system is unfavourable and that acrylates will more or less exclusively bind in their s-*cis* or s-*trans* conformation. The path from such a substrate–enzyme complex to a transition state will be very important for the reaction rate. A substrate–enzyme complex from which a minimal atomic motion is required and in which interactions between the carbonyl oxygen and oxyanion hole can help to break the π system of the substrate would be beneficial.

In this work we investigated the relationship between acrylate conformers bound to the active site and their path to the transition state. We modelled the transition state as a tetrahedral intermediate[10] and evaluated which conformer of the acrylate it could be derived from with minimal atomic motion. Figure 1 shows a modelled tetrahedral intermediate in CALB in which the Oγ of the catalytic S105 and the sp^3-hybridised carbonyl carbon of methyl methacrylate are covalently linked. A minimised structure of the ES complex, which contains free methyl methacrylate, is overlaid on the structure representing the TS. The dihedral angle between the bond vectors connecting the carbonyl oxygen, carbonyl carbon and the unsaturated α- and β-carbon (marked in orange in Figure 1) in the covalently bound substrate defines the conformation of the acry-

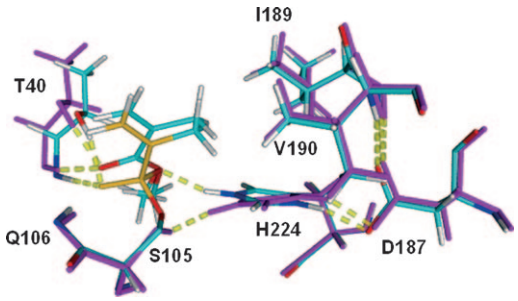

Figure 1. Tetrahedral intermediate, as a representation of the transition state in the acylation of CALB with methyl methacrylate, overlaid on a minimised structure of the ES complex containing free methyl methacrylate. Some atoms are not shown for clarity. The dihedral angle defining the conformation of the covalently bound acrylate substrate (between the carbonyl oxygen, carbonyl carbon and the unsaturated α- and β-carbons) is marked in orange. Colour code: cyan = carbon, red = oxygen, blue = nitrogen, white = hydrogen. The enzyme atoms in the ES-complex are coloured in violet. The two structures were superimposed by using all enzyme atoms with a resulting RMSD of 0.09 Å.

late in the TS. Molecular dynamics simulations were used as a tool to study the enzymatic preference for acrylate conformations in the TS, as described in the Experimental Section. Simulations were performed on wt and mutants of CALB, *Humicola insolens* cutinase (HiC) and *Rhizomucor miehei* lipase (RML) with the three acrylate substrates discussed (methyl acrylate, methyl methacrylate and methyl α-chloroacrylate). The definition of the dihedral angle defining the conformation of enzyme-bound methyl acrylate and methyl α-chloroacrylate was the same as for methyl methacrylate.

The molecular-dynamics simulations resulted in the distribution of acrylate dihedral angles in the TS for CALB-catalysed transacylation shown in Figure 2. The range of possible dihedral angles (from −180° to 180°) was subdivided into intervals of 15° in dihedral angle space. A dihedral angle of −15° to 15° corresponds to an apparent s-*cis* acrylate conformer whereas −165° to −180° and 165° to 180° correspond to an apparent s-*trans* conformer (in the tetrahedral transition state the π system is broken, and thus the term "apparent" is used for the acrylate conformer). We found that the abundance of populations with apparent s-*cis* and s-*trans* conformations was highly dependent on the substrate and the catalyst. CALB wt had a very low abundance of apparent s-*cis* conformers of methyl methacrylate (1.3%) whereas the corresponding number was 17.7% for the more catalytically competent CALB V190A mutant. Methyl acrylate had both apparent s-*cis* and s-*trans* conformers in TS (15.5 and 51.1% abundance, respectively). Thus the faster-reacting substrates and the more potent catalyst displayed a higher abundance of apparent s-*cis*/s-*trans* acrylate conformers in the TS model.

We assumed that only populations with apparent s-*cis*/s-*trans* acrylate conformers in the TS model were productive. This assumption was based on the preference of the substrate for being in a flat conformation. Furthermore, in the computed

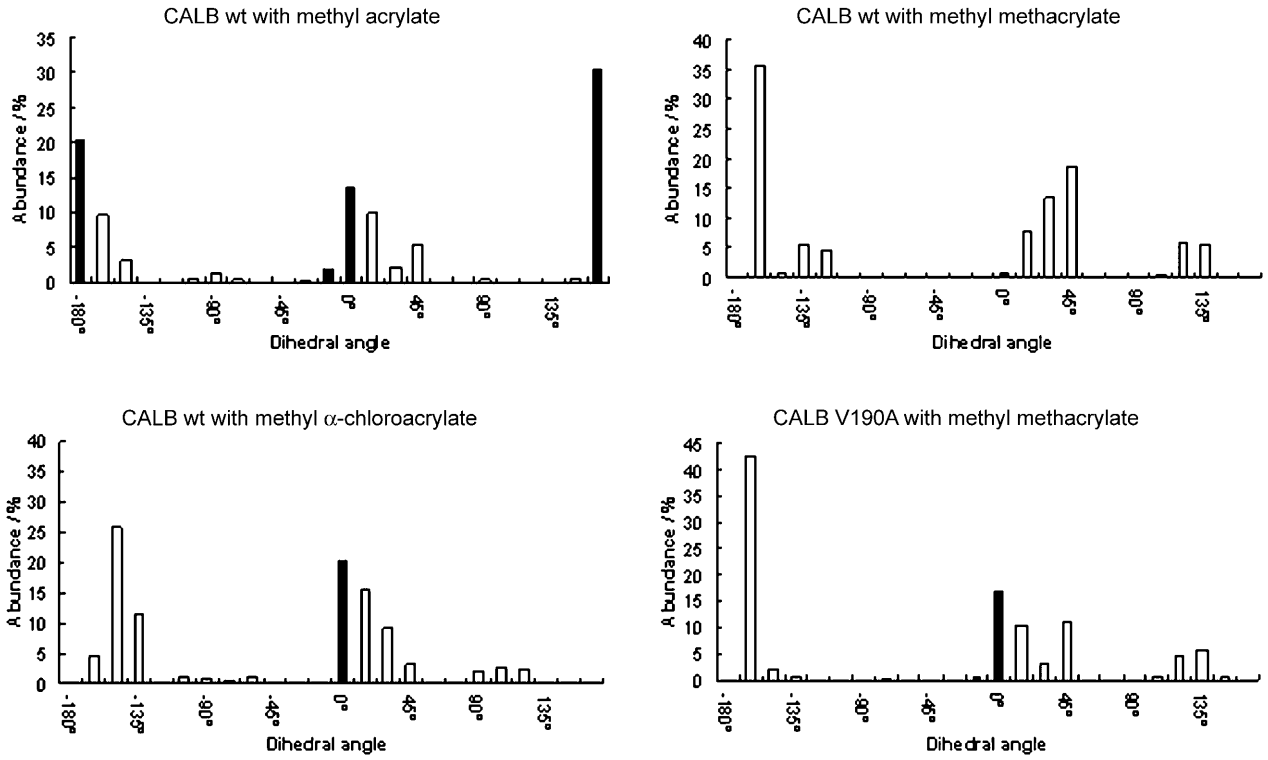

Figure 2. Distribution of acrylate dihedral angles in the TS for enzyme-catalysed transacylation with CALB (the dihedral angle is between the bond vectors connecting the carbonyl oxygen, carbonyl carbon and the α- and β-unsaturated carbon atoms in the enzyme-bound substrate). The dihedral angle space was divided in 15° intervals. Populations with apparent s-*cis* or s-*trans* acrylate conformers (dihedral angles close to 0° and 180°, respectively) are marked in black. The abundance of a certain population was based on the average value from several molecular-dynamics simulations with a minimum of 360 resulting structures.

transition state for acylation of methyl acrylate at the DFT B3LYP 6−31G(d,p) level of theory when using a minimal protein model consisting of a formate ion, an imidazole molecule and a methanol molecule (for the catalytic triad) and two methanol molecules (for the oxyanion hole), methyl acrylate was found to be in a flat conformation (Figure S6).

The relative abundance of productive s-*cis*/s-*trans* transition states obtained from the molecular-dynamics simulation can be translated into total relative probabilities of forming the transition state for each catalyst–substrate pair if the abundances are normalised with the ground-state distribution of substrate conformers. This is because an apparent s-*cis* acrylate conformation in the transition state originates from an s-*cis* ground-state substrate conformation. The relative final probability of forming a productive TS is thus given by the sum of the s-*cis*/s-*trans* population abundance times the concentration of the corresponding free ground-state acrylate conformer (i.e., the concentration of the free s-*cis* or s-*trans* form). This can be expressed as:

$$P_{tot} = A_{TS,s\text{-}cis} \times [\text{s-}cis_{free}] + A_{TS,s\text{-}trans} \times [\text{s-}trans_{free}] \quad (1)$$

Here P_{tot} is the total relative probability of forming a productive TS for the catalyst–substrate pair, $A_{TS,s\text{-}cis}$ and $A_{TS,s\text{-}trans}$ refer to the abundance of productive s-*cis*/s-*trans* transition states obtained from the molecular dynamics simulations, respectively, and the terms within squared brackets refer to the concentrations of free substrate conformers. The result from these calculations are shown in Table 3.

A good linear correlation between experimentally obtained k_{cat} values and the relative probabilities of forming transition states was found, as shown in Figure S7. The slope of the fitted line was found to be 1700 min^{-1}, and the intercept was 64 min^{-1} with an R^2 of 0.99. We tested this model by making the CALB mutant V190L. This mutant was predicted to have a low relative abundance of s-*cis* populations of methyl methacrylate in the TS by modelling. This was in agreement with a measured apparent k_{cat} of 50 min^{-1}.Clearly there is a preference for acrylates to react in their low-energy s-*cis* or s-*trans* ground-state conformations in enzymatic transacylation reactions with CALB.

The simple model for CALB based on assumed productive conformations described above was refined by including the interaction energy between enzyme and substrate in the transition state. The average force field interaction energy between the acrylate substrate and enzyme in the TS was calculated for each population of dihedral angles. Further, the average dihedral angle was used to account for deviations from apparent s-*cis* and s-*trans* substrate conformations in the TS, bearing in mind that the substrate in the transition state originated from an sp^2-hybridised precursor. The sum of the average interaction energy and the cost of distorting the π system were used to assign an energy score to each population (Supporting Information). We assigned populations with productive transition states to be those of lowest energy score or within 1 kcal mol^{-1} of that value. The results of these calculations are shown in Table 4 for wt and mutant CALB where the abundance of productive s-*cis*/s-*trans* populations are given separately (see also Table S7).

Table 3. Relative abundances of populations with apparent s-*cis* and s-*trans* acrylate conformations in the transition-state model and the corresponding total relative probabilities of forming transition state for CALB. The average abundances from several molecular dynamics simulations are shown.[a]

Catalyst	Substrate	Average abundance of s-*cis* populations[b]	Average abundance of s-*trans* populations[b]	Relative probability of forming productive TS[c]
wt	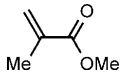	0.013	0	0.003
V190A	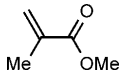	0.177	0	0.048
wt	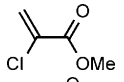	0.202	0	0.117
wt	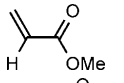	0.155	0.511	0.251
V190A	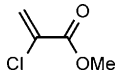	0.478	0	0.277
Test of model				
V190L[d]	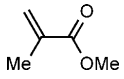	0.003	0	0.001

[a] Based on a minimum of 360 structures from the molecular-dynamics simulation. We assumed that populations with apparent s-*cis*/s-*trans* acrylate conformers were productive. The data are shown according to increasing probability of forming the transition state. [b] The average abundances were based on (from top to bottom): two simulations with a total of 720 generated structures, three simulations with 1440 generated structures, one simulation with 720 structures, two simulations with 1440 structures, two simulations with 720 generated structures, one simulation with 360 generated structures. [c] Corrected for the ground-state conformational distribution of free acrylate as given in Table 2 and by using Equation (1). [d] The V190L mutant with methyl methacrylate was used for evaluation.

It could be concluded that productive populations had an apparent s-*cis* or s-*trans* acrylate conformer in the TS (or a conformation very close to apparent s-*cis*/s-*trans*, Table S7). In most cases, populations with apparent s-*cis* conformations were found to have the lowest energy score. A good correlation between the experimentally determined apparent k_{cat} values and the relative probability of forming productive transition states obtained from modelling and by evaluating the energy score was found for CALB, as shown in Figure 3. Our assumption about productive populations was thus concluded to be fair for CALB.

The correlation between experimental results and modelling was also analysed for *Humicola insolens* cutinase and *Rhizomucor miehei* lipase (Table S8). Productive populations were chosen based on energy score and were translated into relative probabilities of forming transition states by correcting for the ground-state distribution of acrylate conformers, as described for CALB. For HiC, the correlation between experimental results and relative probabilities of forming productive tran-

Table 4. Relative probabilities of forming productive transition states for CALB wt and mutants based on energy score. Productive conformations were those of lowest energy score or within 1 kcal mol^{-1} of that value.

Catalyst	Substrate	Average abundance of productive s-*cis* populations	Average abundance of productive s-*trans* populations	Relative probability of forming productive TS[a]
wt	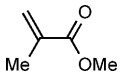	0.013	0	0.003
V190A	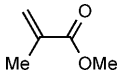	0.277	0.004	0.078
wt	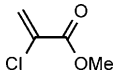	0.202	0	0.117
V190A	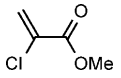	0.435	0	0.253
wt	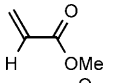	0.182	0.543	0.279
V190L	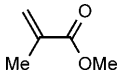	0.006	0	0.0016

[a] Corrected for the ground-state conformational distribution of free acrylate as given in Table 2 and by using Equation (1).

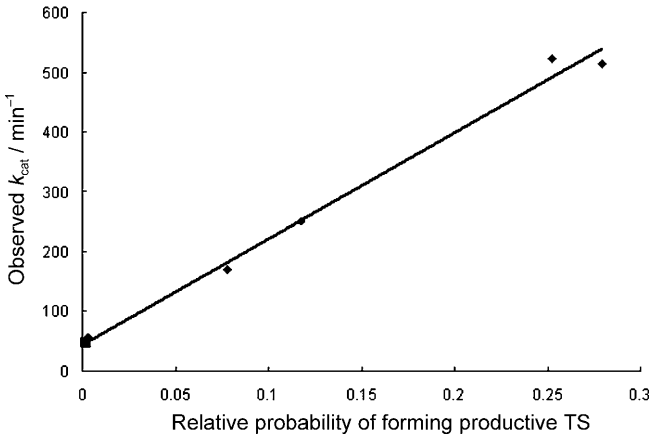

Figure 3. Correlation between experimentally determined k_{cat} values and the relative probabilities of forming productive transition states for CALB wt and mutants (◆) based on the data in Table 4. The productive conformations were those with the lowest energy scores or those within 1 kcal mol^{-1} of that value. V190L, with a measured k_{cat} of 50 min^{-1} with methyl methacrylate (■), was used for evaluation. The linear regression resulted in a line with a slope of 1772 min^{-1}and an intercept of 44 min^{-1} with an R^2 value of 0.99.

sition states was linear with a slope of 2400 min^{-1} and an intercept of 74 min^{-1} with an R^2 of 0.99 (Figure S8). For RML, the correlation was not good, although the productive populations were found to consist of apparent s-*cis*/s-*trans* acrylate conformations. The chlorine in methyl α-chloroacrylate interacted with the $-NH_2$ group of Asn264 through weak electrostatic interactions during the simulation, thus giving a low frequency of productive transition states and a suboptimal fit for this system. Corresponding interactions between the chlorine and CALB or HiC were not possible (in CALB, Gln157 was hydrogen bonded to Asp134 during the course of the simulation and the $-NH_2$ group of Asn67 was pointing the wrong way for HiC).

The importance of the oxyanion hole was clearly seen throughout the molecular-dynamics simulations. Three hydrogen bonds involving the backbones of Leu145 and Ser82 as well as the side chain of Ser82 were formed for RML after Asp91 swung away during the course of the simulation (Asp91 is hydrogen bonded to Ser82 in the crystal structure of the activated enzyme, as described in the literature[11]). Similarly, three hydrogen bonds were formed in the oxyanion hole for CALB and HiC. No difference in hydrogen bond lengths and patterns in the oxyanion hole were discovered for the different acrylate substrates.

The results were consistent with our hypothesis that populations with productive transition states have the covalently bound substrate in an apparent s-*cis* or s-*trans* conformation linked to the enzyme–substrate complex through a minimal motion of atoms.

Discussion

The presence of the π system in acrylates stabilises two flat conformations of the free substrate. Our calculated relative distributions of the low-energy s-*cis* and s-*trans* conformers of methyl acrylate and methyl methacrylate are in good agreement with published data.[12] Our computed energies required for breaking the π system in the free acrylate substrates are of the same order of magnitude as the reported activation barrier of 6 kcal mol^{-1} for s-*cis*/s-*trans* isomerisation of butadiene.[13] Upon placing the acrylate in an enzyme active site, interactions between the substrate and enzyme as well as the aforementioned stabilising interactions in the substrate will affect catalysis. Serine proteases, like lipases, belong to the hydrolase family of enzymes and have a catalytic triad. By studying serine proteases, knowledge about lipases can be gained.

In serine proteases, the substrate's scissile peptide bond is stabilised by π interactions similar to the stabilisation of acrylates. By using ab initio QM/MM calculations on trypsin (EC 3.4.21.4), this bond was found to be only slightly distorted from planarity (dihedral angle of 162.7°) in the tetrahedral intermediate for acylation.[14] A distortion of 29° from planarity was found in the ES complex with an associated energy cost of 1.3 kcal mol^{-1}. Upon formation of tetrahedral intermediate, a rotation of the substrate main-chain NH was observed to prepare for hydrogen transfer from the catalytic histidine and cleavage of the C-terminal peptide segment. Ground-state destabilisation was concluded to be a factor of little catalytic importance.

Similar results were found for the deacylation reaction of porcine pancreatic elastase (EC 3.4.21.36) when using ab initio QM/MM calculations.[15] How do serine proteases provide a driving force for catalysis to occur and how can such knowledge be applied to enzymatic acryltransfer? A shortening of hydrogen bonds in the antiparallel β-sheet formed between substrate and enzyme, optimisation of the hydrogen-bonding pattern in the oxyanion hole and an economy of atomic

motion have been observed upon transition from Michaelis complex to acyl enzyme in serine proteases.[16]

Clearly the oxyanion hole is important and probably required as a driving force to break the π system present in acrylates. The oxyanion hole as driving force for enzymatic acryltransfer can perhaps be used to explain the intriguing fact that acrylates are stabilised by a π system worth close to 6 kcal mol^{-1} with an expected 10^4 reduction in reaction rate compared to the corresponding saturated substrates. Acrylates, however, display a V_{max} only 6–75 times lower than that of the saturated ester methyl propionate.

There are several examples of how substrate binding energy can be used by enzymes to distort the substrate and drive catalysis. One example is the thiamine diphosphate-dependent enzyme transketolase (EC 2.2.1.1) from *Escherichia coli*. It was found that the newly formed covalent bond between the cofactor and C2 of the substrate xylulose 5-phosphate shows significant out-of-plane tension (by 25–30° from the plane formed by the thiazolium ring).[17] This tension is removed upon formation of the enamine intermediate. It should be noted that transketolase uses 11 hydrogen bonds to create the strained intermediate and to funnel binding energy into catalysis. For acrylates, the acyl part of the substrate lacks such hydrogen-bonding possibilities and thus hydrogen bonds cannot be used to create strained acrylate conformers in enzyme-catalysed transacylation. We believe that deviations from unstrained s-*cis* and s-*trans* acrylate conformations is unfavourable in enzyme-catalysed acryltransfer.

Insight into atomic motion during ES-to-TS transitions can be found in the vast amount of structural data deposited in the Protein Data Bank. A number of recently determined crystal structures of trypsin with natural substrates have been used to follow the enzymatic reaction from ES complex to acyl enzyme.[18] Figure 4 shows overlays of representative ES complexes and covalent enzyme–substrate adducts for trypsin and CALB.

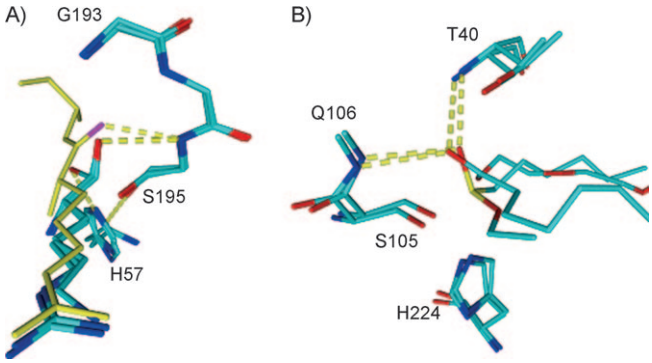

Figure 4. Overlap of representative structures of ES complexes, tetrahedral intermediates and acyl enzymes for A) trypsin and B) CALB. A) ES complex with Alzheimer's Aβ protein precursor (APPI) coloured in yellow with the carbonyl oxygen in magenta and with A15 and R16 shown (PDB ID: 1TAW), the tetrahedral intermediate is with leupeptin (R3 shown, PDB ID: 2AGI), and acyl enzymes are with succinyl-Ala-Ala-Pro-Arg (PDB ID: 2AGE) and succinyl-Ala-Ala-Pro-Lys (PDB ID: 2AGG, has reached further towards deacylation) with R5/K5 shown. B) ES complex with Tween 80 (PDB ID: 1LBT) and tetrahedral intermediate with *n*-hexylphosphonate ethyl ester (PDB ID: 1LBS). The catalytic serine, histidine and oxyanion hole is shown in each case. Colour code: cyan = carbon, red = oxygen, blue = nitrogen. The structures were superimposed by using all enzyme backbone atoms with RMSDs of 0.39 Å for trypsin and 0.36 Å for CALB.

An important conclusion that can be drawn from the crystal structures is that the carbonyl sp^2-to-sp^3 transition seems to take place by a least-motion mechanism similar to the one described, for example, for the thiamine diphosphate-dependent enzyme benzoyl formate decarboxylase (EC 4.1.1.7).[19] This economy in atomic motion can be seen for porcine pancreatic elastase as well when the deacylation is followed.[20] The migration of an electrophilic centre towards an enzyme-activated nucleophile has been described in the literature.[21]

From Figure 4 it seems as though the α-carbon is quite fixed as the reaction proceeds. For trypsin, the Oγ–C–O group in the acyl enzyme occupies essentially the same position in space as in the tetrahedral intermediate. Thus the leaving group (methoxy for methyl esters) seems to be more flexible. The ES complex containing free methyl methacrylate depicted in Figure 1 may be seen in the light of the least-motion mechanism. In fact the free acrylate substrate depicted in Figure 1 is positioned for attack by the catalytic serine with an Oγ–C distance of 3 Å and an Oγ–C–O angle of 96°, in good agreement with the Bürgi–Dunitz trajectory,[22] and can thus be seen as a near-attack (or reactive) complex. Two hydrogen bonds to the oxyanion hole are already formed, and upon transition to the tetrahedral intermediate, a third can be formed to drive catalysis. With the background of the least-motion mechanism, the tetrahedral transition state for enzymatic transacylation of acrylates can be traced back to the corresponding reactive complex between enzyme and sp^2-hybridised acrylate due to the fact that the substrate acyl part seems to be essentially fixed during the catalytic transition. In fact, the good agreement between the experimentally determined apparent k_{cat} values and the probability of forming productive transition states (based on a scoring function that takes deviations from optimal π-overlap in the substrate in the transition state into account) is highly supportive of a least-motion mechanism. Our calculated probabilities of forming productive transition states can thus be translated into probabilities of forming productive near-attack complexes between enzyme and acrylate substrate, bearing the effect of the least-motion mechanism upon the sp^2-to-sp^3 transition in mind. Reactive substrate conformations have been termed near-attack conformers (NACs), and the higher probability of forming such conformations in enzymes compared to in solution have been proposed to influence enzyme efficiency.[23]

The conclusion that acrylates react with very small deviations from their low-energy ground-state conformers s-*cis*/s-*trans* in CALB, HiC and for RML is indicative of the generality of the process. The fact that the correlation between experimental results and modelling is not good for RML might be explained by the fact that this enzyme contains a mobile lid. The presence of a lid can influence the working mode of enzymes (conformational selection vs. induced fit) since certain lid conformations exclude the substrate from the active site.[24] The enzymatic acryltransfer described in this work is dependant both on a conformational selection on the substrate level and on a productive interaction between enzyme and substrate.

Ground-state substrate conformations have previously been shown to affect catalysis, as was the case for enzymatic ring-opening polymerisation with CALB; here the lactone conformation (*cisoid* or *transoid*) was shown to dictate reactivity.[25]

The slope of the line obtained when k_{cat} is plotted against simulation data (Figure 3 for CALB) can be interpreted in terms of the maximum possible k_{cat} (as the intercept is negligible). This corresponds to a situation in which the relative probability of forming a productive transition state is 100%. For CALB, this slope is 1770 min^{-1} and for *Humicola insolens* cutinase the corresponding value is 2400 min^{-1}. Interestingly, this value is close to the k_{cat} value for enzyme-catalysed transacylation of the saturated substrate methyl propionate (apparent $k_{cat}=$ 2000 min^{-1} for CALB and 1000 min^{-1} for HiC). The enzymatic contribution expressed as k_{cat} per probability unit of forming TS (the slope of the line) was thus found to be essentially the same for the different acrylates and methyl propionate, but the probabilities of forming productive transition states were different; this explains the differences in barrier height for the different substrates.

Perhaps this finding is not so surprising because the substrates use the same catalytic machinery, and methyl propionate is a saturated ester with similar carbon skeleton compared to the acrylate substrates investigated in this work. The higher catalytic competency of our rationally designed CALB V190A mutant[26] towards methyl methacrylate can now be explained in the light of the findings in this work. This mutant accommodates s-*cis* conformations of methyl methacrylate better in the active site than does the wt enzyme, thus leading to a higher probability of productive transition state formation.

Conclusions

Free acrylates exist solely in the two low-energy conformations s-*cis*/s-*trans* due to a stabilising π system. Therefore enzyme catalysis depends on starting from these conformers for the formation of productive transition states. We found a correlation between the measured reaction rate and the ability of the catalyst to accommodate apparent s-*cis*/s-*trans* acrylate conformations in the transition state for CALB. This was confirmed by energy evaluation of the populations of different acrylate dihedral angles for CALB and HiC. The results were supportive of a least-motion mechanism with minimal atomic motion during the transition from ES complex to tetrahedral intermediate. Other acrylate conformers than the apparent s-*cis*/s-*trans* conformations in the transition state would involve more atomic motion and would thus violate the least-motion mechanism and make such transition states less productive.

Experimental Section

Chemicals and enzymes: Methyl propionate, propan-1-ol, dodecane, methyl acrylate and methyl methacrylate of $\geq$99% purity were purchased from Sigma-Aldrich. Methyl α-chloroacrylate ($\geq$99%), stabilised with hydroquinone, was from Acros Organics. Diisopropyl ether ($\geq$99%) was from AppliChem (Darmstadt, Germany).

The preparation of CALB wt and mutants is described in detail elsewhere.[26] Briefly, the QuikChange protocol from Stratagene was used to introduce the V190A and V190L mutations into the CALB wt gene in a pGAPz$\alpha\beta$ plasmid. The mutated plasmid DNA was transformed by heat-shock into *E. coli* XL1Blue cells according to the QuikChange protocol. After confirmation of the mutated genes by sequencing, the plasmids were electroporated into *Pichia pastoris* SMD1168H and expressed, together with wt, in BMGY medium (1% yeast extract, 2% peptone, 100 mM potassium phosphate, 1.34% yeast nitrogen base with ammonium sulfate without amino acids, 0.4 mg L^{-1} (4×10^{-5}%) biotin, 1% glycerol, pH 6.0) at 30 °C and 200 rpm. Purification was done by hydrophobic interaction chromatography by using butyl-Sepharose packed in an XK16 column and an ÄKTA explorer (GE Healthcare).

Humicola insolens cutinase wt was a kind gift from Novozymes (Bagsvaerd, Denmark). Immobilised *Rhizomucor miehei* lipase was purchased from Sigma–Aldrich. HiC and CALB wt and mutants were immobilised on Accurel MP 1000 < 1500 micron (Accurel Systems, Sunnyvale, CA, USA), as described in detail elsewhere.[26]

Kinetic measurements: We complemented our previous kinetic experiments[26] with additional measurements and averaged the results. The apparent k_{cat} for enzymatic transacylation of methyl propionate, methyl acrylate, methyl methacrylate and methyl α-chloroacrylate was measured at 30 °C in diisopropyl ether as solvent with propan-1-ol (25 mM) as nucleophile and dodecane (2.5 mM) as internal standard. Typically, the substrate concentration was varied from 50 mM to bulk conditions. The apparent k_{cat} values were calculated by fitting the experimental data to pseudo-one-substrate Michaelis–Menten kinetics by using nonlinear regression in the solver function of Microsoft Excel 2003. At least six points were used to create a Michaelis–Menten curve. For RML and HiC, the apparent k_{cat} value was calculated from the reaction rate in bulk (from at least two separate reactions). The substrate turnover never exceeded 10% conversion. The reaction volume was 2 mL in glass tubes with screw lids. All glassware was dried at 250 °C prior to use, and chemicals were dried on molecular sieves (3 Å, Sigma–Aldrich). The temperature was kept constant at 30 °C, and the stirring speed at 100 rpm by using an HLC heat block. Typically Accurel MP 1000 (10 mg) with immobilised enzyme (ca. 1 nmol active site) was used for each reaction. HiC wt, CALB wt and mutants were equilibrated under LiCl(s) in a desiccator to obtain a water activity of 0.11 prior to reaction (the enzyme was allowed to equilibrate for at least one week).

Samples from the reactions were diluted in diisopropyl ether, and the amount of product (propyl ester) was determined by GC analysis on a HP 5890 Series II Gas Chromatograph (Agilent Technologies, Santa Clara, CA, USA). GC columns were Varian Chrompack Capillary columns, WCOT fused silica, 25 m × 0.32 mm in diameter, CP Chirasil-DEX CB, DF = 0.25 and Chrompack WCOT fused silica 25 m × 0.32 mm in diameter, CP-SIL 5CB, DF = 1.2.

Computational Methods

Calculations to obtain the distribution of ground-state acrylate conformers were performed by using the B3LYP hybrid density functional[27] as implemented in the Gaussian 03 package.[28] Geometry optimisations were carried out at the 6−31G(d,p) level of theory. Final energies were calculated by using a larger basis set, 6−311+G(2d,2p). The effect of solvation was taken into account by performing single-point calculations on the optimised structures by using the CPCM polarisable continuum model[29] with diethyl ether ($\varepsilon = 4.335$) as solvent and adding the resulting value to the

final energies. Diethyl ether was chosen for the calculations because the solvent parameters are readily available. We considered diethyl ether to be a good approximation for diisopropyl ether in which the kinetic experiments were analysed. All structures were verified to be either minima or transitions states by means of vibrational analysis at the same level of theory as for the optimisation. Final energies were corrected for zero-point vibrational effects.

The cost of distorting the acrylate π system in the free substrate was calculated by performing single-point DFT B3LYP 6−31G(d,p) calculations on distorted conformations. Starting from the geometry-optimised s-*cis*/s-*trans* conformations of the acrylates, the dihedral angle defining the distortion of the π system was changed in 15° intervals, and single-point calculations were performed on the resulting structures by using HyperChem.[30] The B3LYP 6−31G(d,p) single-point calculations resulted in a correlation between the energy E and the dihedral angle ϕ between the carbonyl and α,β-double bonds in the acrylate of the type $E = A \times \sin^2(180^\circ - \phi - B)$, where A and B are constants (Supporting Information).

The transition-state geometry for acylation of methyl acrylate in the minimal protein model was calculated by using US-GAMESS 12 JAN 2009 (R3)[31] on a UNIX cluster with nine nodes and ten processors. To simulate a minimal lipase active site, we chose to represent the catalytic triad by a formate ion, an imidazole molecule and a methanol molecule. The oxyanion hole was represented by two methanol molecules. The coordinates of the catalytic triad from PDB ID: 1LBT (CALB with Tween 80) were used as a starting point. The transition-state geometry was first obtained at the HF 6−31G(d) level of theory and then refined (and verified) at the DFT B3LYP 6−31G(d,p) level of theory.

Interactions between enzyme and substrate in the transition state were accounted for by molecular-dynamics simulations. Starting structures of the tetrahedral intermediate as a representation of the TS were prepared for CALB, HiC and RML by using YASARA version 8.9.23.[32] For CALB, PDB 1TCA was used as starting structure and for RML PDB 4TGL (with the lid open) was used. As there is no crystal structure for HiC in the Protein Data Bank, an homology model was prepared by using the SWISS-MODEL homology modelling server.[33] The published alignment of the amino acid sequences from *Fusarium solani* cutinase and HiC was used.[34] PDB 1CEX of *Fusarium solani* cutinase at 1.0 Å resolution was used as template for the homology model. An overlay of the resulting model structure of HiC with *Fusarium solani* cutinase PDB ID: 1XZL using all backbone atoms resulted in an RMSD of 0.55 Å.

Sugars (for CALB) and the inhibitor diethyl phosphonate (for RML) were deleted. All missing hydrogens were added to the three hydrolase structures, and the hydrogen network was optimised by repeated minimisations and short dynamics runs (1200 fs at 298 K) with the Amber99 force field.[35] The tetrahedral intermediate was built as a representation of the TS with the guidance of published binding modes of substrates in the active sites of lipases.[36] The energy-minimised, free acrylate substrates (methyl acrylate, methyl methacrylate and methyl α-chloroacrylate) were prepared in YASARA by using the AUTOSMILES approach[37] and were covalently attached to the catalytic serine in the enzyme (Ser105 in CALB, Ser103 in HiC and Ser144 in RML). The catalytic histidine was protonated, the resulting tetrahedral intermediate was minimised by using Amber99, and a molecular dynamics simulation was run on the covalent enzyme–substrate complex for at least 2 ps at 298 K with PME for long-range electrostatics.[38] The minimisation/molecular dynamics simulation was allowed to proceed until the oxyanion hole was clearly established (with at least two hydrogen bonds formed) and the hydrogen bonds in the catalytic triad formed (between the catalytic D–H and H–S).

The prepared enzyme structures containing covalently attached acrylate substrates were subjected to the conformational search algorithm described in detail in the Supporting Information. Briefly, the dihedral angle in the covalently bound acrylate was subjected to variation, and the whole enzyme–substrate structure was subjected to cycles of minimisation, dynamics for 2 ps at 298 K, and minimisation. The resulting structures were subdivided into populations based on their acrylate dihedral angle (angle between the bond vectors connecting the carbonyl oxygen, carbonyl carbon and the α- and β-unsaturated carbons in the covalently bound substrate in the TS). Each population spanned 15° in dihedral angle space (−180° to −165°, −165° to −150°, −150° to −135°, etc.), thus giving a total of 24 populations, each with different relative abundance. Each population was assigned an energy score that depended on two factors: 1) The average potential energy of the acrylate substrate in the TS (including the acyl group) and 2) The average acrylate dihedral angle in the TS and the associated energy price that needs to be paid for a distorted π system (bearing in mind that the tetrahedral intermediate originated from an sp^2-hybridised acrylate precursor). Structures that did not have at least two hydrogen bonds in the oxyanion hole and one hydrogen bond between the catalytic histidine and enzyme–substrate adduct were not considered. The populations of lowest energy score or within 1 kcal mol^{-1} of that value were assigned as populations with productive transition states.

Acknowledgements

BASF (Ludwigshafen, Germany) is gratefully acknowledged for financial support. Special thanks go to Prof. Fahmi Himo and Dr. Tommaso Marcelli for all their help with the ab initio calculations and fruitful discussions.

Keywords: acrylate · biocatalysis · enzymes · molecular modeling · protein design

[1] a) T. Ohrui, Y. Sakakibara, Y. Aono, M. Kato, H. Takao, T. Kawaguchi, *US Patent 3,875,212* **1975**; b) N. Andoh, I. Nishiwaki, M. Arakawa, *US Patent 4,329,492* **1982**.
[2] U. T. Bornscheuer, K. Buchholz, *Eng. Life. Sci.* **2005**, *5*, 309 – 323.
[3] A. B. Hajjar, P. F. Nicks, C. J. Knowles, *Biotechnol. Lett.* **1990**, *12*, 825 – 830.
[4] S. Warwel, G. Steinke, M. R. Klaas, *Biotechnol. Tech.* **1996**, *10*, 283 – 286.
[5] W. Paulus, B. Hauer, D. Haring, F. Dietsche, US Patent 2006030013 (A1) 2006.
[6] a) M. Nordblad, P. Adlercreutz, *J. Biotechnol.* **2008**, *133*, 127 – 133; b) M. Nordblad, P. Adlercreutz, *Biotechnol. Bioeng.* **2008**, *99*, 1518 – 1524.
[7] T. Tsuji, H. Ito, H. Takeuchi, S. Konaka, *J. Mol. Struct.* **1999**, *475*, 55 – 63.
[8] E. Fisher, *Dtsch. Chem. Ges.* **1894**, *27*, 2984 – 2993.
[9] D. Ringe, G. A. Petsko, *Science* **2008**, *320*, 1428 – 1429.
[10] C.-H. Hu, T. Brinck, K. Hult, *Int. J. Quantum Chem.* **1998**, *69*, 89 – 103.
[11] U. Derewenda, A. M. Brzozowski, D. M. Lawson, Z. S. Derewenda, *Biochemistry* **1992**, *31*, 1532 – 1541.
[12] T. Egawa, S. Maekawa, H. Fujiwara, H. Takeuchi, S. Konaka, *J. Mol. Struct.* **1995**, *352/353*, 193 – 201.
[13] L. Guidoni, U. Rothlisberger, *J. Chem. Theory Comput.* **2005**, *1*, 554 – 560.
[14] T. Ishida, S. Kato, *J. Am. Chem. Soc.* **2003**, *125*, 12035 – 12048.
[15] M. Topf, W. G. Richards, *J. Am. Chem. Soc.* **2004**, *126*, 14631 – 14641.
[16] K. Fodor, V. Harmat, R. Neutze, L. Szilágyi, L. Gráf, G. Katona, *Biochemistry* **2006**, *45*, 2114 – 2121.

[17] P. Asztalos, C. Parthier, R. Golbik, M. Kleinschmidt, G. Hübner, M. S. Weiss, R. Friedemann, G. Wille, K. Tittmann, *Biochemistry* **2007**, *46*, 12037 – 12052.
[18] E. S. Radisky, J. M. Lee, C.-J. K. Lu, D. E. Koshland, Jr., *Proc. Natl. Acad. Sci. USA* **2006**, *103*, 6835 – 6840.
[19] M. Bruning, M. Berheide, D. Meyer, R. Golbik, H. Bartunik, A. Liese, K. Tittmann, *Biochemistry* **2009**, *48*, 3258 – 3268.
[20] R. C. Wilmouth, K. Edman, R. Neutze, P. A. Wright, I. J. Clifton, T. R. Schneider, C. J. Schofield, J. Hajdu, *Nat. Struct. Biol.* **2001**, *8*, 689 – 694.
[21] V. L. Schramm, W. Shi, *Curr. Opin. Struct. Biol.* **2001**, *11*, 657 – 665.
[22] a) H. B. Bürgi, J. D. Dunitz, J.-M. Lehn, G. Wipff, *Tetrahedron* **1974**, *30*, 1563 – 1572; b) H. B. Bürgi, J. D. Dunitz, E. Shefter, *Acta Crystallogr. Sect. B: Struct. Sci.* **1974**, *30*, 1517 – 1527.
[23] T. C. Bruice, P. Y. Bruice, *J. Am. Chem. Soc.* **2005**, *127*, 12478 – 12479.
[24] S. M. Sullivan, T. Holyoak, *Proc. Natl. Acad. Sci. USA* **2008**, *105*, 13829 – 13834.
[25] M. Veld, L. Fransson, A. Palmans, E. W. Meijer, K. Hult, *ChemBioChem* **2009**, *10*, 1330 – 1334.
[26] P.-O. Syrén, E. Lindgren, H. W. Hoeffken, C. Branneby, S. Maurer, B. Hauer, K. Hult, *J. Mol. Catal. B: Enzym.* **2010**; DOI: 10.1016/j.molcatb.2009.11.016.
[27] a) C. Lee, W. Yang, R. G. Parr, *Phys. Rev. B: Condens. Matter Mater. Phys.* **1988**, *37*, 785 – 789; b) A. D. Becke, *Phys. Rev. A: At. Mol. Opt. Phys.* **1988**, *38*, 3098 – 3100; c) A. D. Becke, *J. Chem. Phys.* **1992**, *96*, 2155 – 2160; d) A. D. Becke, *J. Chem. Phys.* **1992**, *97*, 9173 – 9177; e) A. D. Becke, *J. Chem. Phys.* **1993**, *98*, 5648 – 5652.
[28] Gaussian 03 (Revision D.01), Gaussian Inc., Pittsburgh, PA, **2004**.
[29] a) M. Cossi, N. Rega, G. Scalmani, V. Barone, *J. Comput. Chem.* **2003**, *24*, 669 – 681; b) V. Barone, M. Cossi, *J. Phys. Chem. A* **1998**, *102*, 1995 – 2001.
[30] HyperChem ProRelease 7.5, Hypercube Inc., Ontario, Canada, **2003**.
[31] M. W. Schmidt, K. K. Baldridge, J. A. Boatz, S. T. Elbert, M. S. Gordon, J. J. Jensen, S. Koseki, N. Matsunaga, K. A. Nguyen, S. Su, T. L. Windus, M. Dupuis, J. A. Montgomery, *J. Comput. Chem.* **1993**, *14*, 1347 – 1363.
[32] E. Krieger, T. Darden, S. B. Nabuurs, A. Finkelstein, G. Vriend, *Proteins: Struct. Funct. Bioinf.* **2004**, *57*, 678 – 683.
[33] a) K. Arnold, L. Bordoli, J. Kopp, T. Schwede, *Bioinformatics* **2006**, *22*, 195 – 201; b) T. Schwede, J. Kopp, N. Guex, M. C. Peitsch, *Nucleic Acids Res.* **2003**, *31*, 3381 – 3385; c) N. Guex, M. C. Peitsch, *Electrophoresis* **1997**, *18*, 2714 – 2723.
[34] T. Ternstrom, A. Svendsen, M. Akke, P. Adlercreutz, *Biochim. Biophys. Acta Proteins Proteomics* **2005**, *1748*, 74 – 83.
[35] J. Wang, P. Cieplak, P. A. Kollman, *J. Comput. Chem.* **2000**, *21*, 1049 – 1074.
[36] J. Pleiss, M. Fischer, R. D. Schmid, *Chem. Phys. Lipids* **1998**, *93*, 67 – 80.
[37] A. Jakalian, D. B. Jack, C. I. Bayly, *J. Comput. Chem.* **2002**, *23*, 1623 – 1641.
[38] U. Essmann, L. Perera, M. L. Berkowitz, T. Darden, H. Lee, L. G. Pedersen, *J. Chem. Phys.* **1995**, *103*, 8577 – 8593.

Received: December 11, 2009
Published online on March 18, 2010

